Article

Inherent Chirality Dominates the Visible/Near-Ultraviolet CD Spectrum of Rhodopsin

Gennaro Pescitelli, Narasimha Sreerama, Piero Salvadori, Koji Nakanishi, Nina Berova, and Robert W. Woody

J. Am. Chem. Soc., **2008**, 130 (19), 6170-6181 • DOI: 10.1021/ja711009y • Publication Date (Web): 18 April 2008

J|A|C|S
ARTICLES

Published on Web 04/18/2008

Inherent Chirality Dominates the Visible/Near-Ultraviolet CD Spectrum of Rhodopsin

Gennaro Pescitelli,[†] Narasimha Sreerama,[‡] Piero Salvadori,[†] Koji Nakanishi,[§] Nina Berova,[*,§] and Robert W. Woody[*,‡]

Dipartimento di Chimica e Chimica Industriale, Università degli Studi di Pisa, via Risorgimento 35, I-56126 Pisa, Italy, Department of Biochemistry and Molecular Biology, Colorado State University, Fort Collins, Colorado 80523, and Department of Chemistry, Columbia University, 3000 Broadway, MC 3114, New York 10027

Received December 11, 2007; E-mail: rww@lamar.colostate.edu; ndb1@columbia.edu

Abstract: The visible (α) and near-UV (β) CD bands of rhodopsin have been studied extensively, but their source(s) have never been definitively established. Do they result from the intrinsic chirality of the polyene chromophore of the protonated Schiff base of retinal (retPSB) or from the coupling of the transitions of this chromophore with those of protein groups? We have calculated the contributions of these two mechanisms to the CD of rhodopsin. The intrinsic CD of the retPSB chromophore was calculated using time-dependent density functional theory (TDDFT) and, for comparison, the semiempirical ZINDO method. First-order perturbation theory was used to calculate the effects of coupling of the retPSB transitions with the $\pi\pi^*$ transitions of the aromatic chromophores and the $\pi\pi^*$ and $n\pi^*$ transitions of the peptide groups in rhodopsin. Calculations were performed for eight structures based upon the two molecules in the asymmetric unit of four crystal structures. The most reliable results were obtained from TDDFT calculations on the structure of Okada et al. (*J. Mol. Biol.* **2004**, *342*, 571), PDB 1U19. Averaging over the two molecules in the asymmetric unit, the intrinsic rotational strengths are 0.62 $\pm$ 0.00 DBM (Debye−Bohr magneton) and 0.90 $\pm$ 0.03 DBM for the α- and β-bands, respectively. The contributions from coupling with protein groups are, respectively, −0.32 $\pm$ 0.05 and −0.01 $\pm$ 0.03 DBM. Our results show that the visible/near-UV CD bands of rhodopsin are determined by the intrinsic chirality of the retPSB chromophore and that the contributions of coupling with the protein are significantly smaller for the α-band and negligible for the β-band.

Introduction

The circular dichroism spectrum of rhodopsin has been investigated extensively, both experimentally[1–20] and theoretically.[3,6,21–24] The visible and near-UV CD spectrum of rhodopsin has two prominent positive bands associated with the well-known absorption bands of the protonated 11-*cis* retinal Schiff base (retPSB) chromophore: the α-band at 500 nm and the β-band at 335 nm. The intensities of these bands vary with the species and with the solution conditions, especially the nature of the detergent used for solubilizing the protein. However, for

[†] Università degli Studi di Pisa.
[‡] Colorado State University.
[§] Columbia University.

(1) Crescitelli, F.; Mommaerts, W. F. M. H.; Shaw, T. I. *Proc. Natl. Acad. Sci. U.S.A.* **1966**, *56*, 1729–1734.
(2) Kito, Y.; Azuma, M.; Maeda, Y. *Biochim. Biophys. Acta* **1968**, *154*, 352–359.
(3) Waggoner, A. S.; Stryer, L. *Biochemistry* **1971**, *10*, 3250–3254.
(4) Burke, M. J.; Pratt, D. C.; Faulkner, T. R.; Moscowitz, A. *Exp. Eye Res.* **1973**, *17*, 557–572.
(5) Ebrey, T. G.; Yoshizawa, T. *Exp. Eye Res.* **1973**, *17*, 545–556.
(6) Kropf, A.; Whittenberger, B. P.; Goff, S. P.; Waggoner, A. S. *Exp. Eye Res.* **1973**, *17*, 591–606.
(7) Azuma, K.; Azuma, M.; Suzuki, T. *Biochim. Biophys. Acta* **1975**, *393*, 520–530.
(8) Waddell, W. H.; Yudd, A. P.; Nakanishi, K. *J. Am. Chem. Soc.* **1976**, *98*, 238–239.
(9) Shichida, Y.; Tokunaga, F.; Yoshizawa, T. *Biochim. Biophys. Acta* **1978**, *504*, 413–430.
(10) Horiuchi, S.; Tokunaga, F.; Yoshizawa, T. *Biochim. Biophys. Acta* **1980**, *591*, 445–457.
(11) Wagner, J.; Smith, E.; Cusanovich, M. A. *Photochem. Photobiol.* **1981**, *33*, 929–932.
(12) Fukada, Y.; Shichida, Y.; Yoshizawa, T.; Ito, M.; Kodama, A.; Tsukida, K. *Biochemistry* **1984**, *23*, 5826–5832.
(13) Ito, M.; Katsuta, Y.; Imamoto, Y.; Shichida, Y.; Yoshizawa, T. *Photochem. Photobiol.* **1992**, *56*, 915–919.
(14) Hu, S.; Franklin, P. J.; Wang, J.; Ruiz Silva, B. E.; Derguini, F.; Nakanishi, K.; Chen, A. H. *Biochemistry* **1994**, *33*, 408–416.
(15) Suzuki, T.; Makino, M.; Azuma, M. *Biochim. Biophys. Acta* **1977**, *494*, 115–125.
(16) Wada, A.; Sakai, M.; Imamoto, Y.; Shichida, Y.; Yamauchi, M.; Ito, M. *J. Chem. Soc., Perkin Trans. 1* **1997**, 1773–1777.
(17) Tan, Q.; Lou, J.; Borhan, B.; Karnaukhova, E.; Berova, N.; Nakanishi, K. *Angew. Chem., Int. Ed.* **1997**, *36*, 2089–2093.
(18) Lou, J.; Hashimoto, M.; Berova, N.; Nakanishi, K. *Org. Lett.* **1999**, *1*, 51–54.
(19) Fujimoto, Y.; Ishihara, J.; Maki, S.; Fujioka, N.; Wang, T.; Furuta, T.; Fishkin, N.; Borhan, B.; Berova, N.; Nakanishi, K. *Chem.—Eur. J.* **2001**, *7*, 4198–4204.
(20) Fishkin, N.; Berova, N.; Nakanishi, K. *Chem. Record* **2004**, *4*, 120–135.
(21) Honig, B.; Kahn, P.; Ebrey, T. G. *Biochemistry* **1973**, *12*, 1637–1643.
(22) Kakitani, H.; Kakitani, T.; Yomosa, S. *J. Phys. Soc. Jpn.* **1977**, *42*, 996–1004.
(23) Buss, V.; Kolster, K.; Terstegen, F.; Vahrenhorst, R. *Angew. Chem., Int. Ed.* **1998**, *37*, 1893–1895.
(24) Buss, V. *Chirality* **2001**, *13*, 13–23.

 10.1021/ja711009y CCC: $40.75

bovine rhodopsin, typical values[3,4,25] of $\Delta\epsilon_{max}$ are $+10$ M^{-1} cm^{-1} for the α-band and $+20$ M^{-1} cm^{-1} for the β-band, with rotational strengths of 0.5 and 0.8 DBM (1 Debye−Bohr magneton $= 0.9273 \times 10^{-38}$ cgs units $= 0.197$ atomic units), respectively.

The main aim of the present contribution is to establish the source of the retPSB CD bands, a topic that has been discussed extensively in the past but not resolved. The isolated chromophore is achiral and therefore exhibits no CD spectrum. From the earliest studies of rhodopsin CD, two mechanisms have been recognized for CD induced in retPSB by the protein. (1) The retPSB is bound in a chiral conformation, and thus the chromophore is inherently dissymmetric.[26] (2) The retPSB chromophore transitions interact with electronic transitions in the aromatic and peptide groups of the protein.[27,28] Each study has chosen to focus on one or the other of these mechanisms, but all have recognized that both mechanisms probably contribute to the induced CD. The question has been which, if either, is dominant. This problem is addressed in this work by means of quantum-mechanical calculations on retPSB followed by the evaluation of the coupling between chromophore transitions and protein groups, based on first-order perturbation theory.

The mechanism of coupling between aromatic side-chain transitions and retPSB was investigated by Waggoner and Stryer[3] and Kropf et al.[6] In the absence of information about the protein structure, these studies were confined to calculations for hypothetical geometries of, for example, a Trp side chain interacting with the retPSB chromophore. In a related study, Johnston and Zand[29] calculated the rotational strength of the α-band of an all-*trans*-retinylidene Schiff base with a chiral naphthylamine. The studies of rhodopsin and naphthylamine models showed that coupled-oscillator interactions between aromatic and retPSB chromophores can generate rotational strengths comparable to those observed.

Most investigations of rhodopsin CD have concentrated on the chirality of the bound chromophore, i.e., the inherent dissymmetry of retPSB as it is bound in rhodopsin. Steric conflicts imposed by the β-ionone ring, the 11-*cis* bond, and the C5-, C9-, and C13-methyls of the retPSB (Scheme 1) preclude a completely planar conformation. In solution, the molecule exists as racemic pairs of twisted conformers in rapid equilibrium on the time scale of optical spectroscopy. Honig et al.[21] argued that the protein binding site accommodates a narrow range of chiral conformers and is very unlikely to bind an enantiomeric pair. This has been corroborated by the X-ray structure of rhodopsin,[30–34] which reveals a distinctly chiral retPSB.

If the rhodopsin visible/near-UV CD spectrum is dominated by the chirality of the retPSB chromophore, it should be possible

Scheme 1.

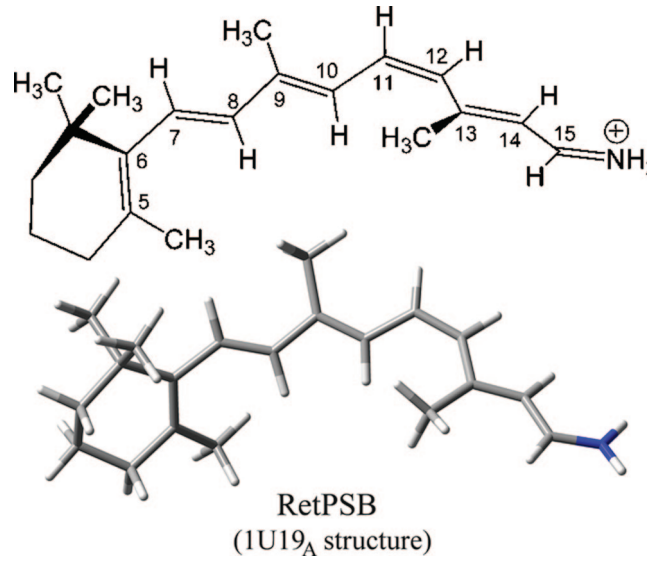

to deduce the conformation of the retPSB by using model compounds, by theoretical calculations on retPSB, or a combination thereof. In fact, many of the previous CD studies on rhodopsin were aimed at determining one or more torsional angles as the main determinant of the observed spectral features. The first theoretical studies[4,21] did not try to deduce specific conformational features but showed that plausibly twisted PSB chromophores could generate rotational strengths comparable to those observed. Kakitani et al.,[22] using π-electron calculations, proposed a specific range of conformations for the retPSB chromophores that would best fit the observed wavelengths, oscillator strengths, and rotational strengths of the α- and β-bands. This led them to propose a 6s-*cis*, 11-*cis*, 12s-*trans* conformation with torsional angles $\tau_{6,7}$ of $-40°$ to $-120°$, $\tau_{11,12}$ of 30° to 40°, and $\tau_{12,13}$ of $-130°$ to $-150°$. (Torsional angles in this paper are defined according to IUPAC conventions.) This conformation is consistent with the X-ray structure of rhodopsin[30–34] with respect to $\tau_{6,7}$ but not with regard to $\tau_{11,12}$ and $\tau_{12,13}$.

More recently, the torsion angles about the C6/C7 and C12/C13 bonds have been examined by experimental studies of the binding of modified retinals to opsin by Ito and co-workers[13,16,35] as well as Nakanishi and co-workers[17–20,36] and by ab initio MO calculations by Buss and co-workers.[23,24,37] Fujimoto et al.[19] showed that, of a pair of enantiomeric derivatives with a five-membered ring connecting C7 and C1 of 11-*cis* retinal, only one enantiomer binds to the opsin. The CD spectrum of the rhodopsin reconstituted with this modified retinal has, like native rhodopsin, positive α- and β-bands, although the magnitudes are smaller by factors of 2 to 3. This derivative has the C6/C7 bond locked in the s-*cis* conformation, and the enantiomer that binds to opsin has $\tau_{6,7} < 0$.

Other retinal analogues have been employed to define $\tau_{12,13}$. The exciton chirality method was applied to 11,12-dihydroretinal[17] and led to the conclusion that $\tau_{12,13}$ is negative. However, Buss and co-workers [23,24] reached the opposite conclusion from

(25) Parkes, J. H.; Rockey, J. H.; Liebman, P. A. *Biochim. Biophys. Acta* **1976**, *428*, 1–12.
(26) Moffitt, W.; Moscowitz, A. *J. Chem. Phys.* **1959**, *30*, 648–660.
(27) Kirkwood, J. G. *J. Chem. Phys.* **1937**, *5*, 479–491.
(28) Tinoco, I. *Adv. Chem. Phys.* **1962**, *4*, 113–160.
(29) Johnston, E. M.; Zand, R. *Biochemistry* **1973**, *12*, 4637–4643.
(30) Palczewski, K.; Kumasaka, T.; Hori, T.; Behnke, C. A.; Motoshima, H.; Fox, B. A.; Le Trong, I.; Teller, D. C.; Okada, T.; Stenkamp, R. E.; Yamamoto, M.; Miyano, M. *Science* **2000**, *289*, 739–745.
(31) Okada, T.; Fujiyoshi, Y.; Silow, M.; Navarro, J.; Landau, E. M.; Shichida, Y. *Proc. Natl. Acad. Sci. U.S.A.* **2002**, *99*, 5982–5987.
(32) Okada, T.; Sugihara, M.; Bondar, A. N.; Elstner, M.; Entel, P.; Buss, V. *J. Mol. Biol.* **2004**, *342*, 571–583.
(33) Li, J.; Edwards, P. C.; Burghammer, M.; Villa, C.; Schertler, G. F. X. *J. Mol. Biol.* **2004**, *343*, 1409–1438.
(34) Teller, D. C.; Okada, T.; Behnke, C. A.; Palczewski, K.; Stenkamp, R. E. *Biochemistry* **2001**, *40*, 7761–7772.
(35) Katsuta, Y.; Sakai, M.; Ito, M. *J. Chem. Soc., Perkin Trans. 1* **1993**, 2185–2192.
(36) Fujimoto, Y.; Fishkin, N.; Pescitelli, G.; Decatur, J.; Berova, N.; Nakanishi, K. *J. Am. Chem. Soc.* **2002**, *124*, 7294–7302.
(37) Kampermann, H.; Kolster, K.; Buss, V. *J. Mol. Model.* **2001**, *7*, 132–139.

Table 1. Intrinsic Rotational Strengths and Torsional Angles[a] for RetPSB in Rhodopsin

structure		$R_{\alpha,\text{int}}$[b]	$R_{\beta,\text{int}}$[b]	$\tau_{6,7}$	$\tau_{11,12}$	$\tau_{12,13}$	Ω_{10-15}[c]
1U19[d]	A	0.6356	0.8683	−30.4	−40.5	−173.5	45.6
	B	0.6111	0.9303	−31.9	−35.9	178.5	45.4
	refined[d,i]	*0.7570*	*1.0309*	*−43.0*	*−17.2*	*174.3*	*30.4*
1L9H[e]	A	0.4071	0.6953	−77.3	−0.2	171.4	13.7
	B	0.6503	0.7981	−84.4	0.0	150.2	43.7
	refined[i,j]	*0.5931*	*1.1905*	*−42.8*	*−18.3*	*171.7*	*30.5*
	refined[i,k]	*0.6783*	*0.9743*	*−46.7*	*−13.9*	*170.1*	*20.6*
1F88[f]	A	0.7521	0.4168	−59.7	−0.6	170.4	10.5
	B	0.4099	0.1703	−58.5	−1.8	157.1	24.5
1HZX[g]	A	−0.7026	−0.1265	−56.6	7.9	156.2	-
	B	0.6992	0.2439	−53.0	7.8	151.6	-
1GZM[h]	A	0.6742	0.4227	−55.2	−11.5	173.2	20.1
	B	0.5831	0.3565	−54.1	−13.5	172.0	23.1

[a] Torsional angles are defined according to IUPAC conventions. [b] Intrinsic rotational strengths calculated by TDDFT, DBM. [c] Dihedral angle between the two planes defined by C10−C11−C12 and C13−C14−C15. [d] Okada et al.[32] [e] Okada et al.[31] [f] Palczewski et al.[30] [g] Teller et al.[34] [h] Li et al.[33] [i] X-ray geometry refined with QM/MM calculations: values in italics. [j] Sugihara et al. [92] [k] Fujimoto et al. [57]

semiempirical and ab initio calculations on idealized models of retPSB. A single enantiomer of an 11-*cis*-locked analogue of retinal in which the C11/C12 bond is part of both a seven-membered and a three-membered ring was found to bind to opsin.[18] This analogue was suggested by the observation[38] that a retinal analogue in which the C11/C12 bond is part of a seven-membered ring forms a PSB with opsin that has a CD spectrum similar to that of rhodopsin, with comparable positive α- and β-bands. Although initial molecular modeling studies suggested a negative $\tau_{12,13}$ in the active enantiomer,[18] further work[36,37] showed that $\tau_{12,13}$ is positive in this enantiomer. Thus, the analogue studies indicate a positive value for $\tau_{12,13}$.

The retPSB chromophore geometries considered here were extracted from all available X-ray structures of rhodopsin. The first structure for rhodopsin based on single-crystal X-ray diffraction was reported in 2000 by Palczewski et al.[30] The conformation of the retPSB in this structure (Table 1) is consistent with the results from the solution studies: $\tau_{6,7} \approx -60°$, $\tau_{12,13} \approx +165°$. Subsequent refinements of this structure,[31,34] a structure obtained with improved crystals of the same form,[32] and a structure of a different crystal form[33] have been generally consistent with this initially determined conformation. However, the torsional angles do show significant variation (Table 1), whether this is attributable to refinement methods or to crystal packing effects. For example, $\tau_{6,7}$ varies from −30° in 1U19[32] to −84° in one chain of 1L9H.[31] The torsion at the *cis* double bond, $\tau_{11,12}$, varies from essentially 0° in 1L9H[31] to −38° in 1U19.[32] The torsional angle $\tau_{12,13}$ is positive in all but one case (the retinal of molecule A of 1U19 has $\tau_{12,13} = -173.5$), but in the two most recently determined structures[32,33] $\tau_{12,13}$ is within ±10° of 180°.

Methods

The intrinsic rotational strengths of the protonated Schiff base of retinal were calculated using the ZINDO semiempirical parametrization[39,40] and time-dependent density functional theory (TDDFT).[41–43] Both types of calculations were run utilizing the Gaussian'03 program.[44] Coupling of the retPSB transitions with transitions in the aromatic side chains and in the peptide groups of the backbone was treated by first-order perturbation theory,[28] using transition moments and transition monopoles approximating the transition charge density generated by the ZINDO or TDDFT treatment.

Intrinsic Contributions. The quantum-mechanical estimation of the rotational strength R_a associated with an electronic transition $0 \rightarrow a$ at frequency ν_a derives from either the dipole-length or the dipole-velocity formalism as follows:[45,46]

$$R_a(\text{DL}) = \text{Im}(\boldsymbol{\mu}_{0a} \cdot \mathbf{m}_{a0}) \quad (1)$$

$$R_a(\text{DV}) = (-e\hbar/2\pi m\nu_a)\text{Im}(\nabla_{0a} \cdot \mathbf{m}_{a0}) \quad (2)$$

and requires evaluation of the electric dipole transition moment $\boldsymbol{\mu}_{0a}$ (or transition momentum, through the del operator ∇_{0a}) and the magnetic dipole transition moment $\mathbf{m}_{a0}$. The current implementation of excited-state calculations in Gaussian'03,[44] with any method, directly provides the rotational strengths computed with both gauge formulations for each excitation. Among the many quantum-mechanical methods suitable for CD calculations,[46,47] many have already been employed for excited-state calculations of retinoids,[48] including ZINDO/S and TDDFT.[48–58] Notably, however, the TDDFT studies did not report computed rotational strengths or CD spectra for retPSB (or analogues) in a geometry consistent with the protein-bound chiral conformation, whereas such calculations using other methods have been described.[23,24] This is especially surprising in view of the increasing popularity of the TDDFT method for the calculation of chiroptical properties of organic chromophores,[43] justified by the very favorable accuracy/cost compromise, especially in the context of absolute configurational assignment, e.g., of natural products.[59–76] In particular, some of us have recently developed a so-called solid-state CD/TDDFT

(38) Akita, H.; Tanis, S. P.; Adams, M.; Baloghnair, V.; Nakanishi, K. *J. Am. Chem. Soc.* **1980**, *102*, 6370–6372.
(39) Ridley, J.; Zerner, M. *Theor. Chim. Acta* **1973**, *32*, 111–134.
(40) Ridley, J. E.; Zerner, M. C. *J. Mol. Spectrosc.* **1974**, *50*, 457–473.
(41) Marques, M. A. L.; Gross, E. K. U. Time-Dependent Density Functional Theory. In *A Primer in Density Functional Theory*; Fiolhais, C., Nogueira, F., Marques, M. A. L., Eds.; Springer: Berlin, 2003; pp 144–184.
(42) Gross, E. K. U.; Burke, K. Basics. In *Time-Dependent Density Functional Theory*; Marques, M. A. L., Ullrich, C. A., Nogueira, F., Rubio, A., Burke, K., Gross, E. K. U., Eds.; Springer: Berlin, 2006; pp 1–13.
(43) Rappoport, D.; Furche, F. Excited States and Photochemistry. In *Time-Dependent Density Functional Theory*; Marques, M. A. L., Ullrich, C. A., Nogueira, F., Rubio, A., Burke, K., Gross, E. K. U., Eds.; Springer: Berlin, 2006; pp 337–354..
(44) Frisch, M. J. et al. *Gaussian 03*, revision B.05; Gaussian, Inc.: Wallingford, CT, 2004.
(45) Koslowski, A.; Sreerama, N.; Woody, R. W. Theoretical Approach to Electronic Optical Activity. In *Circular Dichroism - Principles and Applications*; Berova, N., Nakanishi, K., Woody, R. W., Eds.; Wiley-VCH: New York, 2000; pp 55–95.
(46) Crawford, T. *Theor. Chim. Acta* **2006**, *115*, 227–245.
(47) Diedrich, C.; Grimme, S. *J. Phys. Chem. A* **2003**, *107*, 2524–2539.
(48) Silva López, C.; Nieto Faza, O.; López Estévez, S.; De Lera, A. R. *J. Comput. Chem.* **2006**, *27*, 116–123.
(49) Wanko, M.; Hoffmann, M.; Strodel, P.; Koslowski, A.; Thiel, W.; Neese, F.; Frauenheim, T.; Elstner, M. *J. Phys. Chem. B* **2005**, *109*, 3606–3615.
(50) Wanko, M.; Garavelli, M.; Bernardi, F.; Niehaus, T. A.; Frauenheim, T.; Elstner, M. *J. Chem. Phys.* **2004**, *120*, 1674–1692.
(51) Savedra, R. M. L.; Pinto, M. F. S.; Trsic, M. *J. Chem. Phys.* **2006**, *125*, 144901/1–7.
(52) Sun, M.; Ding, Y.; Cui, G.; Liu, Y. *J. Phys. Chem. A* **2007**, *111*, 2946–2950.
(53) Send, R.; Sundholm, D. *J. Phys. Chem. A* **2007**, *111*, 27–33.
(54) Send, R.; Sundholm, D. *Phys. Chem. Chem. Phys.* **2007**, *9*, 2862–2867.
(55) Tachikawa, H.; Kawabata, H. *J. Photochem. Photobiol. B* **2005**, *79*, 191–195.
(56) Vreven, T.; Morokuma, K. *Theor. Chim. Acta* **2003**, *109*, 125–132.
(57) Fujimoto, K.; Hayashi, S.; Hasegawa, J.-Y.; Nakatsuji, H. *J. Chem. Theory Comput.* **2007**, *3*, 605–618.
(58) Gascon, J. A.; Batista, V. S. *Biophys. J.* **2004**, *87*, 2931–2941.
(59) Atodiresei, I.; Zöllinger, M.; Lindel, T.; Fleischhauer, J.; Raabe, G. *Chirality* **2007**, *19*, 542–549.

approach based on TDDFT calculations on solid-state geometries determined by X-ray diffraction,[62–68] the same kind of approach we employ here.

With the aim of filling the gap, we have run TDDFT calculations on retPSB in the bound chiral geometry both to evaluate the intrinsic contribution to the CD of rhodopsin and to generate transition monopoles necessary for estimating the chromophore/protein couplings (see below). ZINDO calculations were also executed to compare TDDFT results with those from a computationally inexpensive but still widely employed method and for the sake of comparison to previous ZDO semiempirical calculations on retinoids.[19,22,23,48]

Previous literature results evidence interesting trends which can be summarized as follows:

(1) Generally speaking, ZINDO and TDDFT methods predict well the first two vertical excitation energies $S_0 \rightarrow S_{1,2}$ of retinoids,[48,51] including retPSB,[49,50,52–54,57,58] when compared with experimental values and/or results obtained with *ab initio* methods like CASSCF/CASPT2 (complete active space self-consistent field/second-order perturbation) or CC2 (second-order approximate coupled-cluster model).[77]

(2) TDDFT-computed excitation energies depend strongly on the functional employed,[48,49,52] the best results being obtained with hybrid functionals like B3LYP (Becke's three-parameter functional);[78] on the other hand, the basis set dependence is less pronounced,[52,55] and the basis set limit seems to be already reached with TZVP, a triple-ζ split-valence basis set with polarization functions (not augmented with diffuse functions).[79]

(3) Similarly, TDDFT-computed oscillator strengths f depend significantly on the functional but less on the basis set.[50,52] Again, hybrid functionals like B3LYP led to the best agreement with CC2 and CASPT2 results.[54,80] B3LYP and CASPT2 values have been found to be consistent with the experimental values obtained from the recently measured photoabsorption spectra of 11-*cis* and all-*trans* retinal Schiff bases.[81]

(4) The ground-state input geometries for the above calculations were obtained in most cases with B3LYP/6-31G(d) optimizations, which led to results in very good agreement with higher-level ones;[49,53,57] the impact of the functional and basis set employed for geometry optimizations is minor.[52]

The overall good performance of TDDFT methods in predicting $S_0 \rightarrow S_{1,2}$ excitation energies and oscillator strengths of retinoids is somewhat surprising when the different character of these two excited states is considered. For retinylidene Schiff bases, in the ground-state S_0 the positive charge is most localized on the imine side of the molecule; the first excited-state S_1 has substantial charge-transfer (hole-pair) character, with the charge predominantly on the β-ionone side, while the second excited-state S_2 is largely covalent, with a charge distribution more similar to that of S_0.[49,50,52,53,80] It is known that TDDFT may not describe with equivalent accuracy excited states with different ionic vs covalent character[50,82,83] and has inherent difficulties with charge-transfer transitions in the commonly employed adiabatic local density approximation, because of the incorrect asymptotic behavior of exchange-correlation functionals.[41,43] In fact, it has been found that, for the charge-transfer S_1 state of retinal (and analog) Schiff bases, the geometry (in terms of bond length alternation), the charge distribution and the dipole moment (in terms of difference $\Delta\mu_{0\rightarrow1}$ with the ground state) are incorrectly predicted with B3LYP.[50] The $\Delta\mu$ value is especially important because it is experimentally available for retPSB[84] and may be easily computed. Most DFT functionals tend to underestimate $\Delta\mu_{0\rightarrow1}$,[49,53,54] but hybrid methods like BH-LYP (Becke's half-and-half-functional)[85] with a large fraction of "exact" exchange character led to the value closest to reference methods,[49] probably because of some compensation effect.

In light of the conclusions above, we chose the BH&HLYP functional[85] with Ahlrich's TZVP[79] basis set for our TDDFT calculations on retPSB. (The BH&HLYP implementation in Gaussian'03 actually adds a B88-type[86] gradient exchange correction to the original BH&H.[85]) The ZINDO/S method and, in one case, B3LYP/TZVP were also employed for comparison. The input structures were generated from all available X-ray structures of rhodopsin, designated by the PDB[87] file names (1U19,[32] 1F88,[30] 1L9H,[31] 1HZX, [34] 1GZM[33]) and the letters A or B (indicated as subscripts) for the two molecules in the asymmetric unit (see Table 1). For each structure, the Lys296 N−Cϵ bond was replaced by a

(60) Frelek, J.; Kowalska, P.; Masnyk, M.; Kazimierski, A.; Korda, A.; Woznica, M.; Chmielewski, M.; Furche, F. *Chem.−Eur. J.* **2007**, *13*, 6732–6744.
(61) Giorgio, E.; Tanaka, K.; Verotta, L.; Nakanishi, K.; Berova, N.; Rosini, C. *Chirality* **2007**, *19*, 434–445.
(62) Hussain, H.; Krohn, K.; Flörke, U.; Schulz, B.; Draeger, S.; Pescitelli, G.; Antus, S.; Kurtán, T. *Eur. J. Org. Chem.* **2007**, 292–295.
(63) Hussain, H.; Krohn, K.; Florke, U.; Schulz, B.; Draeger, S.; Pescitelli, G.; Salvadori, P.; Antus, S.; Kurtan, T. *Tetrahedron: Asymmetry* **2007**, *18*, 925–930.
(64) Krohn, K.; Zia-Ullah; Hussain, H.; Flörke, U.; Schulz, B.; Draeger, S.; Pescitelli, G.; Salvadori, P.; Antus, S.; Kurtán, T. *Chirality* **2007**, *19*, 464–470.
(65) Krohn, K.; Kock, I.; Elsässer, B.; Flörke, U.; Schulz, B.; Draeger, S.; Pescitelli, G.; Antus, S.; Kurtán, T. *Eur. J. Org. Chem.* **2007**, 1123–1129.
(66) Krohn, K.; Farooq, U.; Flörke, U.; Schulz, B.; Draeger, S.; Pescitelli, G.; Salvadori, P.; Antus, S.; Kurtán, T. *Eur. J. Org. Chem.* **2007**, 3206–3211.
(67) Dai, J.; Krohn, K.; Elsässer, B.; Flörke, U.; Draeger, S.; Schulz, B.; Pescitelli, G.; Salvadori, P.; Antus, S.; Kurtán, T. *Eur. J. Org. Chem.* **2007**, 4845–4854.
(68) Kurtán, T.; Pescitelli, G.; Salvadori, P.; Kenéz, Á.; Antus, S.; Szilágyi, L.; Illyés, T.-Z.; Szabó, I. *Chirality* **2008**, *20*, 379–385.
(69) Matsumoto, K.; Inagaki, T.; Nehira, T.; Kannami, M.; Inokuchi, D.; Kurata, H.; Kawase, T.; Pescitelli, G.; Oda, M. *Chem.−Asian J.* **2007**, *2*, 1031–1036.
(70) Stephens, P. J.; Pan, J.-J.; Devlin, F. J.; Urbanova, M.; Hajicek, J. *J. Org. Chem.* **2007**, *72*, 2508–2524.
(71) Stephens, P. J.; Devlin, F. J.; Gasparrini, F.; Ciogli, A.; Spinelli, D.; Cosimelli, B. *J. Org. Chem.* **2007**, *72*, 4707–4715.
(72) Stephens, P. J.; Pan, J. J.; Devlin, F. J.; Krohn, K.; Kurtán, T. *J. Org. Chem.* **2007**, *72*, 3521–3536.
(73) Spassova, M.; Asselberghs, I.; Verbiest, T.; Clays, K.; Botek, E.; Champagne, B. *Chem. Phys. Lett.* **2007**, *439*, 213–218.
(74) Pescitelli, G.; Bari, L. D.; Caporusso, A. M.; Salvadori, P. *Chirality* **2008**, *20*, 393–399.
(75) Bringmann, G.; Maksimenka, K.; Mutanyatta-Comar, J.; Knauer, M.; Bruhn, T. *Tetrahedron* **2007**, *63*, 9810–9824.
(76) Krick, A.; Kehraus, S.; Gerhauser, C.; Klimo, K.; Nieger, M.; Maier, A.; Fiebig, H.-H.; Atodiresei, I.; Raabe, G.; Fleischhauer, J.; Konig, G. M. *J. Nat. Prod.* **2007**, *70*, 353–360.
(77) (a) Andersson, K.; Malmqvist, P.-Å.; Roos, B. O. *J. Chem. Phys.* **1992**, *96*, 1218–1226. (b) Christiansen, O.; Koch, H.; Jorgensen, P. *Chem. Phys. Lett.* **1995**, *243*, 409–418.
(78) Becke, A. D. *J. Chem. Phys.* **1993**, *98*, 5648–5652.
(79) Schafer, A.; Huber, C.; Ahlrichs, R. *J. Chem. Phys.* **1994**, *100*, 5829–5835.
(80) Cembran, A.; Gonzalez-Luque, R.; Altoe, P.; Merchan, M.; Bernardi, F.; Olivucci, M.; Garavelli, M. *J. Phys. Chem. A* **2005**, *109*, 6597–6605.
(81) Nielsen, I. B.; Lammich, L.; Andersen, L. H. *Phys. Rev. Lett.* **2006**, *96*, 018304/1–4.
(82) Parac, M.; Grimme, S. *Chem. Phys.* **2003**, *292*, 11–21.
(83) Grimme, S.; Parac, M. *Phys. Chem. Chem. Phys.* **2003**, *4*, 292–295.
(84) Mathies, R.; Stryer, L. *Proc. Natl. Acad. Sci. U.S.A.* **1976**, *73*, 2169–2173.
(85) Becke, A. D. *J. Chem. Phys.* **1993**, *98*, 1372–1377.
(86) Becke, A. D. *Phys. Rev. A* **1988**, *38*, 3098–3100.
(87) Berman, H. M.; Westbrook, J.; Feng, Z.; Gilliland, G.; Bhat, T. N.; Weissig, H.; Shindyalov, I. N.; Bourne, P. E. *Nucleic Acids Res.* **2000**, *28*, 235–242.
(88) Rassolov, V. A.; Ratner, M. A.; Pople, J. A.; Redfern, P. C.; Curtiss, L. A. *J. Comput. Chem.* **2001**, *22*, 976–984.
(89) Andruniow, T.; Ferre, N.; Olivucci, M. *Proc. Natl. Acad. Sci. U.S.A.* **2004**, *101*, 17908–17913.

Table 2. Vertical Excitation Energies and Oscillator Strengths Calculated for Rhodopsin (Structure $1U19_A$) with Various Methods

	α band			β band				
method	λ (nm)	*E* (eV)	*f*	λ (nm)	*E* (eV)	*f*	ΔE^a (eV)	f^b ratio
BH&HLYP/TZVP	541.9	2.29	1.08	361.9	3.43	0.40	1.14	2.7
B3LYP/TZVP	633.4	1.96	0.72	431.2	2.87	0.59	0.91	1.2
ZINDO	588.3	2.11	1.22	376.6	3.29	0.38	1.18	3.2

[a] Energy gap, $E_\beta - E_\alpha$. [b] f_α/f_β.

NH_2^+ fragment, and then all hydrogens were reoptimized with B3LYP/6-31G(d)[88] while keeping all heavy atoms frozen. TDDFT calculations were run *in vacuo* on the structures thus obtained; the rotational strengths for α and β bands for the 10 X-ray structures are reported in Table 1.

Neglect of the protein field in excited-state calculations for retPSB certainly represents the most drastic of our approximations. This neglect is compensated in part by several factors. (1) The effect of the protein binding site on the chromophore geometry is implicitly taken into account, as the X-ray geometries are employed. (2) The retPSB chromophore is intrinsically chiral,[26] which means that the $\pi\pi^*$ transitions are allowed both magnetically and electrically and are not orthogonally polarized in the isolated chromophore, as is the case with chromophores that are chiral only because of their environment. This makes the rotational strengths much less sensitive to details of the geometry and environment. (3) Literature results indicate that the effects of an external electrostatic field (e.g., from a single point charge or a portion of a protein simulated by the ONIOM-QM/MM model) on TDDFT-computed excitation energies and $\Delta\mu$ values for retPSB are modest.[49,56,57] One reason for these latter results lies perhaps in the observation that the charges associated with the various residues in the protein binding pocket seem to balance each other, globally providing an isolated-like condition for the chromophore.[89,90] Moreover, we are interested in the relative weight of intrinsic and extrinsic effects rather than in their absolute intensities, and it may be expected that the impact of any approximation on these *relative* values is acceptable.

A further possible source of error lies in employing as input structures retPSB geometries taken from single-crystal X-ray diffractions without refinement of the heavy-atom positions. The limited resolution of X-ray structures may introduce small errors in the geometric parameters (distances and angles), which may have in principle some impact on the computed properties.[49] However, among the several applications reported so far of the solid-state TDDFT/CD approach (vide supra),[62–68] only once has a refinement of the X-ray structure led to slightly improved TDDFT-calculated CD spectra.[64] In the current case, because we are interested in the coupling of the chromophore transitions with the aromatic and peptide chromophores throughout the protein, refinement of the chromophore itself or of the chromophore plus its immediate environment would not be sufficient. A correct refinement procedure would necessarily involve the whole protein, e.g., by means of geometry optimizations or molecular dynamics simulations within a QM/MM framework,[91] which would go beyond the scope of the present paper. However, QM/MM-"relaxed" retPSB geometries are available from the literature[32,57,92] for the best resolved X-ray structure (1U19) as well as for a second one (1L9H). These geometries, when used as inputs for TDDFT calculations, gave results that were similar to those obtained with nonrelaxed input geometries (vide infra), thus justifying our approach.

Table 2 reports, for the reference $1U19_A$ structure, BH&HLYP/TZVP, B3LYP/TZVP, and ZINDO/S results for vertical excitation energies and oscillator strengths *f* of the α and β bands, as well as the $\alpha-\beta$ energy gaps and *f* ratios. Overall, BH&HLYP and ZINDO values agree well with each other and with the experimental photoabsorption spectrum in the gas phase for the 11-*cis* retinal Schiff base (energy gap 1.15 eV, estimated *f* ratio ≈ 2.6).[81] In the solution absorption spectra of rhodopsin, the energy gap is similarly around ∼1.17 eV and the *f* ratio is estimated as ∼3.1.[6,22] Moreover, dipole moment differences $\Delta\mu_{01}$ and $\Delta\mu_{02}$ for $S_0 \rightarrow S_{1,2}$ computed by BH&HLYP/TZVP are 15.6 and 6.3 D, respectively. The former value is in good agreement with the experimental ones[84] (12.7 ± 1.4 for 11-*cis* retinal, 12.0 ± 2.0 for protonated all-*trans* retPSB). Also, the S_1 charge distribution obtained with BH&HLYP/TZVP (see Figure S1 in the Supporting Information) is in keeping with CASSCF results on retPSB,[80] while B3LYP performed less well on a short retinal model.[50]

Configuration analysis of BH&HLYP/TZVP results reveal that the α band is mainly associated with the HOMO → LUMO transition, while the β band is primarily (HOMO−1) → LUMO, plus minor contributions from HOMO → LUMO and HOMO → (LUMO+1). The relevant Kohn–Sham orbitals are depicted in Figure 1. With BH&HLYP, both LUMO and LUMO+1 have negative eigenvalues, and the α and β excitation energies are well below the estimated ionization potential (around 9 eV); these are necessary prerequisites for accurate TDDFT excited-state calculations.[93] Rotational strengths computed with the dipole-length gauge were considered (Table 1), in view of their generally observed superior robustness in comparison to dipole-velocity values.[47] Origin-independence is not achieved with the present calculations, which do not employ gauge-independent or London atomic orbitals.[94] However, we verified that with BH&HLYP/TZVP dipole-length and dipole-velocity values for rotational strengths agreed within 5–7% for both α and β bands. With ZINDO, the discrepancy is much larger and may reach 100%, although the sign is never reversed.

Extrinsic (Coupling) Contributions. According to first-order perturbation theory, the contribution of electronic transitions *b* in protein groups *j* to the rotational strength of a transition *a* in a chromophoric group *i* is[28]

$$R_{ia} = -\left\{ 2\sum_{j\neq i}\sum_{b\neq a} \frac{V_{i0a;j0b}}{h(\nu_b^2 - \nu_a^2)}\left[\frac{\pi}{c}\nu_a\nu_b\mathbf{R}_{ij}\cdot\boldsymbol{\mu}_{i0a}\times\boldsymbol{\mu}_{j0b} + \mathrm{Im}(\nu_b\boldsymbol{\mu}_{j0b}\cdot\mathbf{m}_{ia0} + \nu_a\boldsymbol{\mu}_{i0a}\cdot\mathbf{m}_{jb0})\right]\right\} \quad (3)$$

where $V_{i0a;j0b}$ is the energy of interaction of the transition charge density for transition $0 \rightarrow a$ in group *i* with that of $0 \rightarrow b$ in group *j*; ν_a and ν_b are the transition frequencies of the respective transitions; $\boldsymbol{\mu}_{i0a}$ and $\boldsymbol{\mu}_{j0b}$ are the respective electric dipole transition moments for the transitions; $\mathbf{m}_{ia0}$ and $\mathbf{m}_{jb0}$ are the respective magnetic dipole transition moments; and $\mathbf{R}_{ij} = \mathbf{R}_j - \mathbf{R}_i$ is the vector from the center of group *i* to that of group *j*.

The electric and magnetic dipole transition moments were taken from ZINDO or TDDFT calculations, generated by Gaussian'03. The centers of the chromophores were taken to be a point near C8 for retPSB; the center of gravity of the carbon atoms of the Phe

(90) Cembran, A.; Bernardi, F.; Olivucci, M.; Garavelli, M. *J. Am. Chem. Soc.* **2004**, *126*, 16018–16037.
(91) Wanko, M.; Hoffmann, M.; Frauenheim, T.; Elstner, M. *J. Comput.-Aided Mol. Des.* **2006**, *20*, 511–518.
(92) Sugihara, M.; Hufen, J.; Buss, V. *Biochemistry* **2006**, *45*, 801–810.
(93) Casida, M. E.; Jamorski, C.; Casida, K. C.; Salahub, D. R. *J. Chem. Phys.* **1998**, *108*, 4439–4449.
(94) Pecul, M.; Ruud, K.; Helgaker, T. *Chem. Phys. Lett.* **2004**, *388*, 110–119.

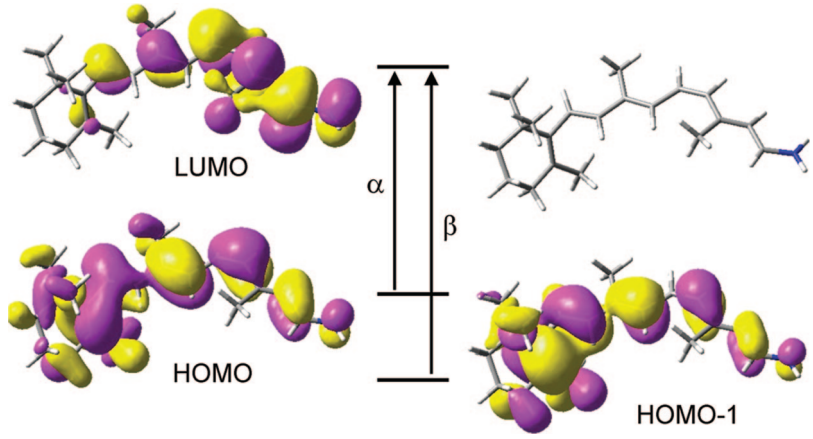

Figure 1. Relevant Kohn–Sham orbitals computed with BH&HLYP/TZVP for retPSB from X-ray 1U19$_A$ geometry. The vertical excitations shown represent the largest contributions to α and β bands.

ring; the center of gravity of the seven heavy atoms for the Tyr ring; the center of the $C_{\delta 2}-C_{\epsilon 2}$ bond for Trp; and the carbonyl carbon for the amide group. These centers were also used in the calculation of the magnetic dipole transition moments.

The interaction of the transition charge densities is approximated by the Coulomb interaction of the sets of point charges representing the two transition charge densities:

$$V_{i0a;j0b} = \sum_s \sum_t \frac{\rho_{i0as}\,\rho_{j0bt}}{|R_{i0as;j0bt}|} \tag{4}$$

where the ρ_{i0as} and ρ_{j0bt} are the transition monopoles defined below, and $|\mathbf{R}_{i0as;j0bt}| = |\mathbf{R}_{j0bt} - \mathbf{R}_{i0as}|$ is the distance between the transition monopole s of $0 \rightarrow a$ and t of $0 \rightarrow b$.

For electrically allowed transitions, i.e., $\pi\pi^*$ transitions, the transition monopoles ρ_{i0as} are defined such that

$$\boldsymbol{\mu}_{i0a} = \sum_s \rho_{i0as}\mathbf{R}_{is} \tag{5}$$

where $\mathbf{R}_{is}$ is the position of atom s, and the sum is over all π-centers in group i. The transition monopoles ρ_{j0bt} are defined in the same way. For the electrically forbidden peptide $n\pi^*$ transition, the monopoles form a quadrupolar charge distribution about the C=O bond with charges and positions as described previously.[95,96]

Two procedures were used to generate the transition monopoles for the $0 \rightarrow \alpha$ and $0 \rightarrow \beta$ transitions of the retPSB chromophore.

(1) ZINDO monopole charges were generated from the ZINDO[39,40] wave functions. The monopole charges for the $0 \rightarrow \alpha$ transition were multiplied by a scaling factor so that they reproduce a transition dipole moment consistent with the experimental oscillator strength[4,97] ($f_\alpha = 0.75$, $\lambda_\alpha = 495$ nm, $\mu_\alpha = 8.89$ D). The same scaling factor (0.7189) was applied to the $0 \rightarrow \beta$ monopoles, giving $\mu_\beta = 3.99$ D, corresponding to a predicted $f_\beta = 0.22$ for an observed wavelength $\lambda_\beta = 345$ nm.[5]

(2) TDDFT monopole charges defined according to Mulliken[98] were calculated by Gaussian'03 for the transition charge densities $0 \rightarrow \alpha$ and $0 \rightarrow \beta$ from the TDDFT wave functions. The Mulliken charges on hydrogen atoms were combined with those on the heavy atom by adjusting the charge on the heavy atom to which they are bonded, using a procedure introduced by Rizzo and Schellman[99] that preserves the total charge (zero) and the transition dipole moment. Rizzo and Schellman used the method to adjust theoretical monopole charges to reproduce an experimental transition dipole moment, but they did not describe it in detail. The program used here, called QADJ, is described and the FORTRAN code is given in the Supporting Information. The TDDFT monopoles were adjusted to reproduce the experimental transition moment magnitudes and the TDDFT transition moment directions.

Calculations of the coupling with aromatic side-chain transitions included four $\pi\pi^*$ transitions for Phe, four for Tyr, and six for Trp. The parameters used were identical to those used by Woody and Sreerama.[96] Coupling to the $n\pi^*$, NV_1, and NV_2 transitions of the amide groups in the peptide backbone also used the parameters of Woody and Sreerama.

Detailed calculations were performed for eight rhodopsin structures, derived from four X-ray crystallographic studies 1U19,[32] 1F88,[30] 1L9H,[31] and 1GZM,[33] each with two molecules in the asymmetric unit. A fifth structure, 1HZX,[34] was briefly considered, but the chromophore conformation in this structure is exceptional, and the intrinsic rotational strengths for the α- and β-bands of molecule A were calculated to be negative (Table 1) so calculations of the coupling contributions were not performed.

Results

Several considerations indicate that our calculations for the 1U19[32] structure using the BH&HYLP/TZVP parameters are the most definitive. (1) The TDDFT method is an *ab initio* method (apart from a few parameters used to define hybrid functionals), in contrast to the semiempirical ZINDO method; moreover, with the latter a great variation was observed between rotational strengths computed with the dipole-length and dipole-velocity formulations. (2) As discussed in the Methods section above, the current combination of functional/basis set is expected to predict the excited states of retPSB with reasonable accuracy (and at a limited computational cost). (3) The 1U19 structure has a higher resolution (2.2 Å) than the 1L9H (2.6 Å), 1F88 (2.8 Å), or 1GZM (2.65 Å) structures. (4) The intrinsic rotational strengths calculated for the two independent molecules in the asymmetric unit agree substantially better for the 1U19 structure than for the lower resolution structures, especially 1F88. (5) Among the calculations for 1U19, the TDDFT results give the best agreement between the A and B molecules. Therefore, we will discuss the BH&HLYP/TZVP results for 1U19 in most detail, and those for the other structures and methods will be described only for purposes of comparison.

Table 1 shows intrinsic rotational strengths calculated for 13 geometries of the retPSB chromophore. The values are remark-

(95) Woody, R. W. *J. Chem. Phys.* **1968**, *49*, 4797–4806.
(96) Woody, R. W.; Sreerama, N. *J. Chem. Phys.* **1999**, *111*, 2844–2845.
(97) Shichi, H.; Lewis, M. S.; Irreverre, F.; Stone, A. L. *J. Biol. Chem.* **1969**, *244*, 529–536.
(98) Mulliken, R. S. *J. Chem. Phys.* **1955**, *23*, 1833–1840.
(99) Rizzo, V.; Schellman, J. A. *Biopolymers* **1984**, *23*, 435–470.

Table 3. Contributions of Coupling with Aromatic and Peptide Groups to Rhodopsin Rotational Strengths for 1U19[a]

structure and method			$R_{\mu\mu}$	$R_{m\mu}$	$R_{\mu m}$	R_{ext}
$1U19_A$ TDDFT (BH&H)	α	Aro	−0.2705	0.2666	−0.0098	−0.0138
		Pep	−0.0453	−0.2040	0.0005	−0.2488
	β	Aro	−0.2426	0.2084	0.0204	−0.0139
		Pep	0.1155	−0.0713	−0.0018	0.0424
$1U19_B$ TDDFT	α	Aro	−0.2569	0.2067	−0.0234	−0.0736
		Pep	−0.1237	−0.1748	0.0018	−0.2967
	β	Aro	−0.2638	0.1604	0.0159	−0.0874
		Pep	0.0983	−0.0573	0.0003	0.0413
$1U19_A$ TDDFT (B3)	α	Aro	−0.2045	0.1452	−0.0140	−0.0734
		Pep	−0.0888	−0.1665	−0.0001	−0.2554
	β	Aro	−0.1790	0.1831	0.0054	0.0095
		Pep	0.0468	−0.1063	0.0002	−0.0593
$1U19_A$ ZINDO	α	Aro	−0.4686	0.2369	−0.0014	−0.2330
		Pep	0.0438	−0.1822	0.0014	−0.1370
	β	Aro	−0.2240	0.0638	0.0443	−0.1159
		Pep	0.1542	−0.0340	−0.0109	0.1093
$1U19_B$ ZINDO	α	Aro	−0.4815	0.1715	−0.0189	−0.3291
		Pep	−0.0446	−0.1620	0.0035	−0.2031
	β	Aro	−0.2758	0.0478	0.0407	−0.1874
		Pep	0.1681	−0.0299	−0.0068	0.1314

[a] First row: aromatic contributions; second row: peptide contributions. The source of the monopole charges is shown in the first column. All rotational strengths are in DBM. For the TDDFT calculations for $1U19_A$, the BH&HLYP functional[85] was compared with the B3LYP functional.[78] $R_{\mu\mu}$, μ-μ coupling; $R_{m\mu}$, m-μ coupling; $R_{\mu m}$, μ-m coupling; R_{ext}, total extrinsic term. See text for explanation.

ably robust in the TDDFT, especially for R_β, with the exception of one structure (1HZX). Averaging over eight X-ray structures (two molecules in each of the four crystal structures 1U19, 1L9H, 1F88, and 1GZM) gives $R_\beta = +0.58 \pm 0.26$ DBM. Structure 1HZX is exceptional in that the C14/C15 bond is strongly twisted ($\tau_{14,15} = -114.3°$ for A, −99.0° for B), while it is nearly planar for all other structures (∼±180°); the same is true for the C13/C14 double bond, which shows twists of $\tau_{13,14} = +36.2°$ for A, +37.7° for B. In fact, $1HZX_A$ is the only geometry for which negative rotational strengths are calculated for both α and β bands, and the transition wavelengths are red-shifted by 200 nm with respect to all other cases. Evidently, the results are strongly affected by the unnatural geometry.

Three sets of values reported in Table 1 were estimated employing retPSB structures obtained from full QM/MM refinements (with different methods) of either the 1U19[32] or 1L9H structure,[57,92] rather than from the X-ray geometry. Some differences in the relevant angles between refined structures and the corresponding unrefined ones are apparent, but the overall geometry is preserved; the rms deviations for the conjugated atoms (from C5 to N) are in fact modest: 0.14 Å for 1U19, 0.23–0.24 Å for 1L9H (considering molecule A). In general, the structural modifications observed after QM/MM "relaxation" of crystal structures of retPSB (and of its binding site) have never been large,[32,58,100] but even minor differences in the input geometries of retinoids may lead to perceptible effects on the predicted properties.[49,57] In the current case, the transition wavelengths and oscillator/rotational strengths for both α- and β-bands obtained for the three refined structures were in good agreement with those for the corresponding unrefined ones (see Table 1).

A comparison of calculated rotational strengths with literature results is possible for structure $1F88_B$ which is similar to that used by Buss et al. as input for CNDO/S, CIS (with 6–31+G(d,p) basis), and CASSCF/CASPT2 calculations.[23] Estimated R_α values with the three methods were +0.4, +2.6, and +1.1 DBM, respectively, which compare well with ours (+0.41 DBM); no calculated R_β values were reported. Buss also reported an R_α value calculated with CASPT2 on the geometry obtained upon QM/MM refinement of X-ray structure 1L9H.[92] It amounts to +3.3 DBM, far from our calculated value (+0.59 DBM) as well as from experiment (∼+0.5 DBM). A further set of CD calculations on retPSB using CIS and CASSCF methods was reported by Buss,[24] but none of the nine input structures employed is consistent with any of ours, so a direct comparison is impossible.

Table 4. Overall Rotational Strengths Calculated for Rhodopsin, Structure 1U19, with Various Methods[a]

structure and method		R_{int}	R_{aro}	R_{pep}	R_{tot}
$1U19_A$ TDDFT (BH&H)	α	0.6356	−0.0138	−0.2488	0.3730
	β	0.8683	−0.0139	0.0424	0.8968
$1U19_A$ TDDFT (B3)	α	0.5967	−0.0734	−0.2554	0.2679
	β	0.5640	0.0095	−0.0593	0.5142
$1U19_B$ TDDFT	α	0.6111	−0.0736	−0.2967	0.2408
	β	0.9303	−0.0874	0.0413	0.8842
$1U19_A$ ZINDO	α	0.8807	−0.2330	−0.1370	0.5107
	β	1.0759	−0.1159	0.1093	1.0693
$1U19_B$ ZINDO	α	0.8957	−0.3291	−0.2031	0.3635
	β	0.9526	−0.1874	0.1314	0.8966

[a] The source of monopole charges is indicated in the first column. All rotational strengths in DBM. The BH&HLYP functional[85] was used in all TDDFT-based calculations except those reported in the third and fourth lines of the table, for which the B3LYP functional[78] was used. R_{int}, intrinsic term; R_{aro}, coupling with aromatic transitions; R_{pep}, coupling with amide transitions; R_{tot}, sum of all terms.

Table 3 shows the contributions of the coupling with the aromatic and peptide groups calculated for the 1U19 structure with the TDDFT (BH&HLYP/TZVP) parameters. The contributions of coupling are combined with the intrinsic rotational strengths for the 1U19 structures to yield the total rotational strengths, given in Table 4. The rotational strengths for molecules A and B were averaged, with the results shown in Table 5; the average coupling with the aromatic side-chain transitions is predicted to contribute -0.04 ± 0.03 DBM to R_α and -0.05 ± 0.04 DBM to R_β. Peptide contributions are calculated to be -0.27 ± 0.02 and $+0.04 \pm 0.00$, respectively. For the α-band, the aromatic and peptide contributions are predicted to be of

(100) Bravaya, K.; Bochenkova, A.; Granovsky, A.; Nemukhin, A. *J. Am. Chem. Soc.* **2007**, *129*, 13035–13042.

Table 5. Rotational Strengths for Rhodopsin Averaged over Molecules A and B of Structure 1U19[a]

method		R_{int}	R_{aro}	R_{pep}	R_{tot}
TDDFT	α	0.6234 ± 0.0022	−0.0437 ± 0.0299	−0.2728 ± 0.0240	0.3069 ± 0.0661
	β	0.8993 ± 0.0310	−0.0507 ± 0.0368	0.0419 ± 0.0006	0.8905 ± 0.0063
ZINDO	α	0.8882 ± 0.0075	−0.2811 ± 0.0481	−0.1701 ± 0.0331	0.4371 ± 0.0736
	β	1.0143 ± 0.0617	−0.1517 ± 0.0358	0.1204 ± 0.0111	0.9830 ± 0.0864

[a] The source of monopole charges is indicated in the first column (BH&HLYP functional employed for TDDFT calculations). The average rotational strength and the rmsd are given. All rotational strengths in DBM. See legend to Table 4.

the same sign and negative, with the peptide contributions nearly an order of magnitude larger. In the case of the β-band, the aromatic and peptide coupling gives contributions of opposite sign, negative and positive, respectively, and of approximately equal and small magnitude. Thus, the coupling effect on the β-band is much smaller than that on the α-band. The smaller energy difference between the β-band and the perturbing aromatic and peptide transitions favors this band over the α-band (eq 3). Noting that the most important perturbing bands are at about 200 nm, this leads to a 2-fold advantage for β over α. However, this is more than compensated by a 7-fold difference arising from the disparity in oscillator strengths, which favors the more intense α-band. Thus, other things being equal, the coupling with the α-band should be about 3.5 times larger than that with the β-band. However, because of differences in the transition moment directions and distribution of transition charge densities, the coupling effects tend to cancel for the β-band and to reinforce for the α-band (see Tables 4 and 5).

Coupling of electric dipole transitions moments in the retPSB with those in aromatic side chains ($\mu-\mu$ coupling) is comparable in importance to coupling of the magnetic transition dipole moment of the retPSB and electric dipole transition moments of the aromatic groups (m$-\mu$ coupling) (Table 3). These are of opposite sign for both the α- and β-bands and this leads to the small resultant contributions from the aromatic transitions. The coupling of the retPSB electric dipole transition with the magnetic dipole transition moments of the aromatic groups ($\mu-$m coupling) is weak, at least an order of magnitude smaller than the $\mu-\mu$ and m$-\mu$ terms, but because of the extensive cancelations of these other terms, the $\mu-$m contribution is comparable to their resultant and therefore is significant. It is negative for the α-band and positive for the β-band.

Which aromatic side chains are most important for the extrinsic CD? Table 6 shows data for the aromatic side chains that have the largest effects in $1U19_A$, listing all those that contribute rotational strengths of ±0.05 DBM or more to either the α- or β-band. With respect to the α-band, Trp 265 at 5 Å (center to center) and Tyr 268 at 4 Å have the largest effect, but significant contributions are found for a few distant side chains (e.g., Trp 35 at 25.5 Å). The contribution of Trp 265 (−0.48 ± 0.04) to R_α is comparable to the intrinsic rotational strength, but this and other negative values are closely balanced by positive contributions. For the β-band, only two side chains contribute more than ±0.05 DBM, Trp 265 at 5 Å and Tyr 191 at 7.5 Å, and these are opposite in sign. Figure 2 shows the retPSB chromophore and the major contributing aromatic side chains for molecule A of the 1U19 structure. Side chains that make a positive contribution to R_α are shown in blue, and those that contribute negative rotational strength are represented in red.

The peptide transitions contribute substantially to the rotational strength of the α-band, with a magnitude nearly half that of the intrinsic rotational strength, and are opposite in sign (Table 4). The contribution to the β-band is, by contrast, about

Table 6. Contributions of Aromatic Side Chains to Rhodopsin Rotational Strengths for 1U19[a]

residue		distance[b]	R_α[c]	R_β[d]
Trp 35	A	25.6	−0.0500	−0.0182
	B	25.7	−0.0518	−0.0176
Trp 126	A	12.8	0.0602	0.0239
	B	12.7	0.0567	0.0182
Tyr 178	A	9.1	−0.0994	−0.0182
	B	9.1	−0.0952	−0.0096
Tyr 191	A	7.6	−0.0297	0.0808
	B	7.1	−0.0286	0.0990
Tyr 192	A	12.2	−0.0790	−0.0332
	B	12.0	−0.0801	−0.0356
Phe 208	A	9.1	0.1237	−0.0106
	B	9.0	0.1231	−0.0199
Phe 212	A	9.5	0.1805	−0.0037
	B	9.5	0.2038	−0.0070
Trp 265	A	5.0	−0.4400	−0.0931
	B	5.0	−0.5128	−0.0985
Tyr 268	A	4.0	0.1994	−0.0096
	B	3.9	0.1256	−0.0630
Phe 293	A	12.3	0.0756	−0.0015
	B	12.4	0.0572	−0.0099

[a] TDDFT monopoles were used. "A" and "B" refer to structures $1U19_A$ and $1U19_B$. [b] Distance between center of aromatic ring system and retPSB (in Å), as specified in text. [c] Contribution to rotational strength of α-band. In DBM. [d] Contribution to rotational strength of β-band. In DBM.

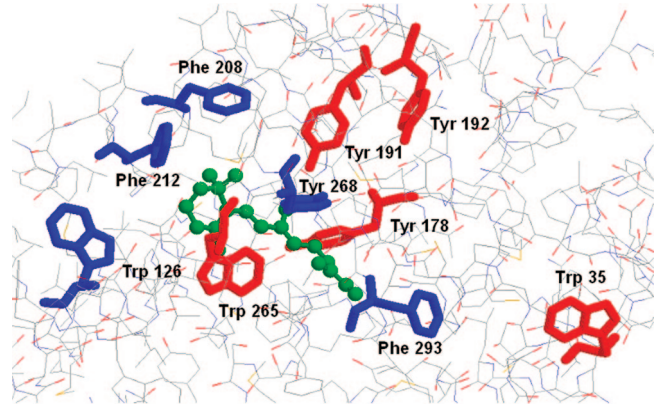

Figure 2. The retPSB chromophore, in green, and the nearby aromatic side chains that contribute most strongly to the induced CD of rhodopsin. Side chains that make positive contributions to R_α are shown in blue. Those that make negative contributions are in red.

5% of the intrinsic rotational strength and of the same sign. The contributions of individual peptides are small, with the largest being <0.02 DBM in magnitude. The $\mu-\mu$ and m$-\mu$ terms are both negative for the α-band, with the m$-\mu$ term larger in magnitude (Table 3). For the β-band, the $\mu-\mu$ and m$-\mu$ terms are opposite in sign and comparable in magnitude, leading to a small resultant. The $\pi\pi^*$ transitions of the amide groups dominate the peptide-induced rotational strength. The $\mu-$m term, arising from the peptide nπ^* transition, makes a negligible contribution to both the α- and β-bands. Tables S1−S3

Table 7. Contributions of Helical and Nonhelical Segments to RetPSB Rotational Strengths in $1U19_A$[a]

segment[b]	residues	band	$R_{\mu\mu}$	$R_{m\mu}$	$R_{\mu m}$	R_{tot}
N-term	1–32	α	−0.0545	−0.0207	0.0000	−0.0751
		β	−0.0401	−0.0008	−0.0003	−0.0412
H-I	33–65	α	−0.0278	0.0144	0.0003	−0.0130
		β	−0.0018	0.0090	0.0002	0.0074
L-I	66–69	α	−0.0055	−0.0006	−0.0001	−0.0062
		β	−0.0001	0.0004	−0.0000	0.0003
H-II	70–101	α	0.0924	0.0933	0.0016	0.1873
		β	−0.0342	0.0463	0.0010	0.0131
L-II	102–104	α	0.0048	−0.0005	0.0001	0.0044
		β	0.0010	−0.0004	−0.0000	0.0006
H-III	105–140	α	−0.0069	−0.0857	0.0005	−0.0922
		β	0.0754	−0.0552	−0.0008	0.0193
L-III	141–148	α	−0.0058	−0.0032	−0.0000	−0.0091
		β	0.0007	−0.0005	−0.0000	0.0002
H-IV	149–173	α	−0.0341	−0.0646	0.0006	−0.0982
		β	0.0360	−0.0376	−0.0000	−0.016
L-IV	174–194	α	0.0626	−0.1042	0.0004	−0.0412
		β	0.0573	−0.0250	−0.0018	0.0306
H-V	195–224	α	0.0405	0.0200	−0.0002	0.0604
		β	0.0060	0.0079	−0.0005	0.0133
L-V	225–240	α	0.0035	−0.0009	0.0000	0.0026
		β	0.0008	0.0000	0.0000	0.0008
H-VI	241–278	α	−0.0101	0.0925	−0.0015	0.0809
		β	−0.0334	0.0293	0.0005	−0.0036
L-VI	279–283	α	−0.0093	−0.0035	−0.0002	−0.0131
		β	−0.0036	0.0006	−0.0000	−0.0031
H-VII	284–309	α	−0.0972	−0.1402	−0.0010	−0.2384
		β	0.0526	−0.0483	0.0000	0.0043
H-VIII	310–322	α	0.0081	0.0016	−0.0000	0.0097
		β	−0.0002	0.0022	−0.0000	0.0020
C-term	323–347	α	−0.0059	−0.0016	−0.0000	−0.0076
		β	−0.0009	0.0009	−0.0000	−0.0000

[a] Rotational strength contributions in DBM. [b] H-I, H-II, etc. denote the helical segments of the protein; L-I, L-II, etc. denote the interhelical loops; N- and C-terminals indicate the respective terminal regions of the polypeptide chain.

(Supporting Information) give the corresponding results for the coupling contributions in structures 1L9H,[31] 1F88,[30] and 1GMZ.[33]

Table 7 shows the contributions of the individual helical and nonhelical segments to the rotational strengths R_α and R_β. The two largest contributors to R_α are helical segments H-II and H-VII, which are in the vicinity of the PSB end of the chromophore (the Lys 296 that forms the PSB is near the center of H-VII). The two helices make contributions to R_α of opposite sign. Significant contributions result from all of the other helices except for H-I and H-VIII, the latter of which is an extramembrane helix approximately orthogonal to the other seven helices. Helices H-IV, H-V, and H-VI are near the β-ionone ring of the chromophore. Helix H-IV makes a negative contribution whereas helices H-V and H-VI provide positive contributions.

Figure 3 shows the helical segments surrounding the PSB chromophore with color coding to show their R_α contributions: red for negative and blue for positive. It is clear that there is no simple pattern to these values, with respect to disposition about the chromophore or with respect to polarity of the helices. For example helices H-II and H-VII are oriented in the opposite N → C sense and make opposite-signed contributions. However, helices H-III and H-IV also have opposite orientations, and both make negative contributions. Of the nonhelical regions, only the NT and L-IV make contributions comparable to those of the helices. These are two of the longest nonhelical regions, and both lie on the extracellular side of the membrane, the side nearest the chromophore.

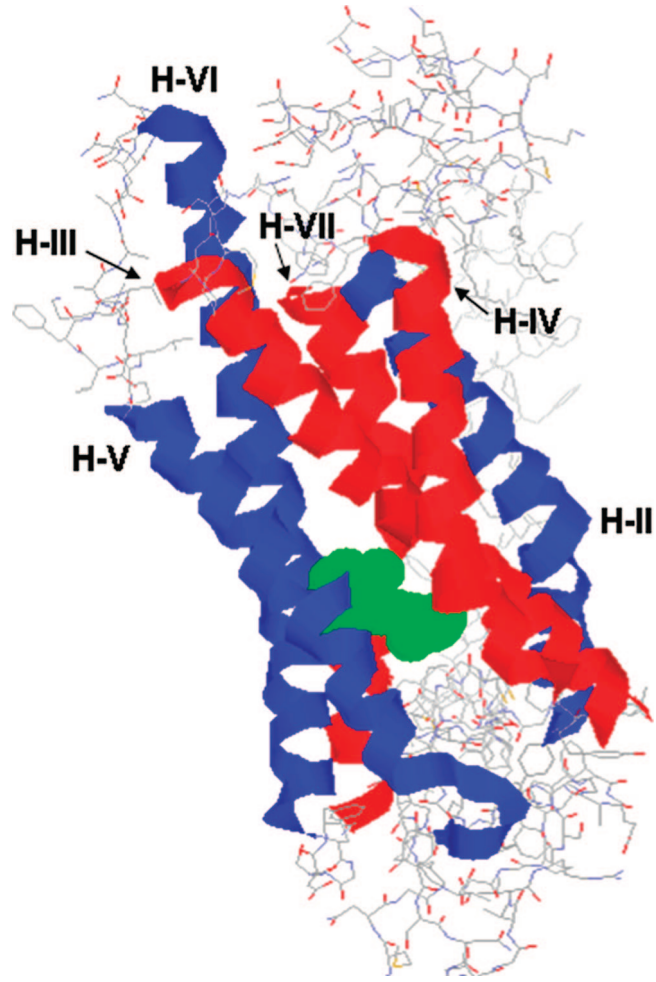

Figure 3. The retPSB chromophore, in green, and the helical segments that contribute most strongly via coupled-oscillator interactions with their peptide transitions to the induced CD of rhodopsin. Helices that make positive contributions to R_α are shown in blue. Those making negative contributions are in red.

Peptide contributions to R_β are uniformly small. The largest is from NT, but this is smaller in magnitude than all but the two weakest helical contributions to R_α. The small values result from the approximate cancelation of the $\mu-\mu$ and m$-\mu$ terms for peptide-β coupling, in contrast to reinforcing terms for R_α.

The extrinsic and intrinsic contributions combine to form the total calculated rotational strengths for molecules A and B. The results for 1U19 are shown in Table 4. The values for the two molecules in the asymmetric unit are in good agreement for the TDDFT (BH&HLYP) calculations, but the ZINDO calculations show a larger discrepancy for molecules A and B. The corresponding data for the 1L9H, 1F88, and 1GZM structures are shown in Tables S4−S6 (Supporting Information), respectively. In these cases, the agreement for the two molecules is generally not as good as that for 1U19, as discussed below. Nevertheless, the averages for each structure have been calculated and are reported in Tables S7−S9 (Supporting Information).

In the TDDFT approach, the total rotational strength, R_{tot}, averaged over molecules A and B in the 1U19 structure, is 0.31 ± 0.07 DBM for the α-band and 0.89 ± 0.01 DBM for the β-band (Table 5). The intrinsic rotational strengths show smaller relative RMSDs than the coupling contributions. However, three of the four coupling terms are small (<∼0.05 DBM in

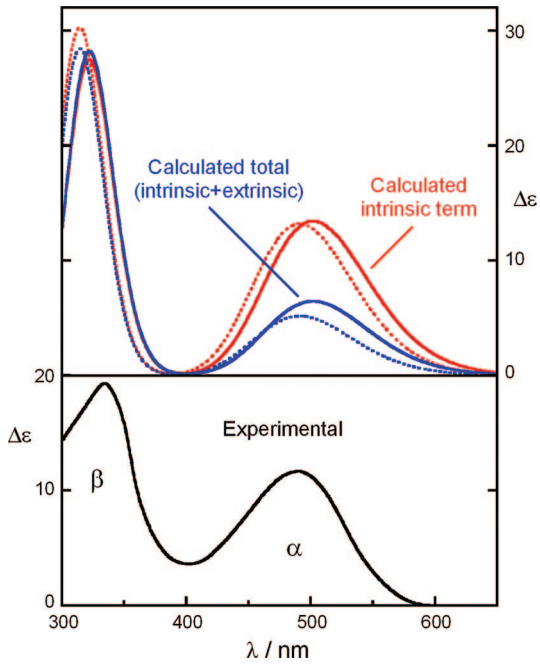

Figure 4. Comparison of calculated and experimental CD spectra of bovine rhodopsin. The calculated spectra (shifted 40 nm to the left) were generated from TDDFT calculations for 1U19, molecules A (solid lines) and B (dotted lines), using dipole-length rotational strengths to which a Gaussian band shape was applied with 3300 cm^{-1} full width at half-height (82.5 nm at 500 nm). Experimental spectrum taken from ref 3.

magnitude), and those for the coupling with aromatic side chains show the largest A/B differences (RMSDs of ~70%), whereas the one sizable coupling term has an rmsd of ~10%.

The predicted rotational strengths from Table 5 agree qualitatively with experiment in that both the α and β bands are calculated to be positive, with the β band significantly more intense. Quantitative comparison shows that the theory underestimates R_α by a factor of 2 (0.31 DBM calculated vs 0.58 observed), but the nearly exact agreement for R_β (0.89 DBM calculated vs 0.84 observed) is better than would be expected. Figure 4 shows a comparison of the calculated and observed CD spectra.

Tables 3−5 also show the results of the ZINDO calculations for 1U19. For both the α- and β-bands, ZINDO gives a larger intrinsic rotational strength for the retPSB chromophore than TDDFT. There are no systematic differences in the aromatic and peptide contributions. The magnitudes of the total rotational strengths are also greater for ZINDO than for TDDFT for both bands.

For the reference structure $1U19_A$, the B3LYP functional was also employed for a full set of calculations to compare with BH&HLYP results. The overall conclusion that the intrinsic contribution is dominant for both bands persists, although some differences are found for some single terms (Tables 3 and 4). For the α-band, the largest difference is that the aromatic coupling makes a more negative contribution. The peptide coupling results are similar to those obtained with BH&HLYP. The intrinsic contribution, which is comparable for the two functionals, prevails. For the β-band, the aromatic and peptide contributions are reversed in sign for the B3LYP functional relative to the BH&HLYP functional. However, these are both relatively small and oppose each other, so the intrinsic term, which is more sensitive to the functional, still strongly prevails over the extrinsic ones.

Tables S7−S9 show the corresponding data for the 1L9H, 1F88, and 1GZM structures, respectively. ZINDO calculations predict larger intrinsic dipole-length and dipole-velocity rotational strengths than TDDFT for the α-band of 1L9H and the β-band of 1F88 and 1GZM, but the converse is true for the β-band of 1L9H and the α-band of 1F88 and 1GZM. The β-band of 1L9H is predicted by ZINDO to have an unusually small rotational strength (0.07 DBM), with both monomers A and B giving small values. The α-band of $1F88_B$ gives anomalous results for both methods: R_α is predicted to be negative. The principal factor in all of these anomalies is an unusually small positive intrinsic rotational strength (e.g., TDDFT gives 0.41 DBM for the α-band of molecule $1F88_B$ vs 0.75 DBM for molecule $1F88_A$). The coupling contributions in these cases are comparable to those for 1U19.

Discussion

The main purpose of this study is to determine the dominant factor in the induced CD of rhodopsin, if any. We find that the intrinsic rotational strength of the retPSB chromophore is the principal determinant of both the α- and β-bands of the rhodopsin CD spectrum. Our most reliable calculations, those using TDDFT transition parameters with the best-resolved structure, 1U19, show that the intrinsic retPSB rotational strength for the α-band is about 2-fold larger than the total from the coupling with aromatic and peptide transitions. This result is even more convincing for the β-band, where the intrinsic term is ~30-fold larger than the coupling terms. Although the uncertainty is larger for the ZINDO parameters and lower resolution structures, the conclusions are consistently the same for all structures and methods considered.

The intrinsic rotational strengths of the retPSB chromophore calculated for eight geometries from the 1U19, 1L9H, 1F88, and 1GZM crystal structures reveal relatively modest variations especially for the α-band, despite significant variations in some torsional angles of the structures, as shown in Table 1.

Previous studies have suggested that the intrinsic rotational strengths of the retPSB can be correlated with torsion about specific bonds in the polyene chain. Shichida et al.[9] suggested that the absence of a β-band and a normal α-band in the CD spectra of rhodopsin analogues reconstituted with 5,6-dihydroretinal[6] and 5,6-epoxy-3-dehydroretinal[101] is evidence that the β-band is sensitive to the torsion about the C6/C7 bond. Fukada et al.[12] have studied a rhodopsin in which the retinal has the 11-*cis* bond locked in a five-membered ring, thus enforcing planarity on the polyene chain from C9 to C14. This analogue has no detectable CD in the α-band but has a normal β-band in CD. Fukada et al. argued that this implies that the α-band CD primarily reflects torsion about the C12/C13 bond. The *ab initio* calculations of Buss and co-workers[23,24] indicated that the sign of the α-band correlates with the sign of $\tau_{12,13}$ but that positive $\tau_{6,7}$ torsion contributes positive rotational strength to the α-band and negative rotational strength to the β-band. However, Buss considered the concentration on the torsion about these two bonds as oversimplified and pointed out[24] that the effects of polyene nonplanarity on the CD are likely to be additive. These views are in agreement with our results.

Table 1 compiles the calculated intrinsic rotational strengths together with the values for the three torsional angles that have

(101) Azuma, M.; Azuma, K.; Kito, Y. *Biochim. Biophys. Acta* **1973**, *295*, 520–527.

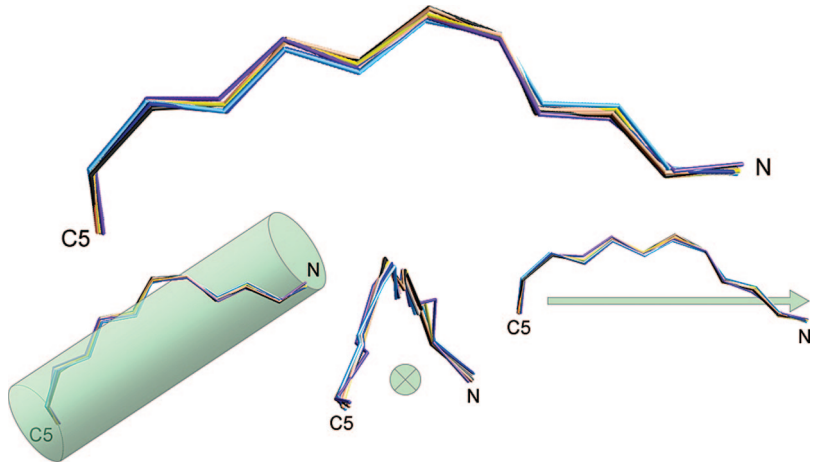

Figure 5. Top: Best rms fit of the conjugated skeleton of retPSB in eight structures (color code: black, $1U19_A$; brown, $1U19_B$; gray, 1U19 refined by Okada et al.; violet, $1L9H_A$; blue, 1L9H refined by Sugihara et al.; light blue, 1L9H refined by Fujimoto et al.; orange, $1GZM_A$; yellow, $1GZM_B$; see Table 1 for references). Bottom: overall helicity defined by the conjugated skeleton; from left to right: right-handed helicity emphasized; view along helix main axis, from C5 viewpoint; view from direction perpendicular to helix axis.

been considered critical for the intrinsic CD[13,22–24] ($\tau_{6,7}$, $\tau_{11,12}$, and $\tau_{12,13}$) in the structures studied. The calculated rotational strengths do not appear to correlate with any of the three angles. For example, the results for $1L9H_B$ agree well with those for both molecules of the 1U19 structure, despite the fact that $\tau_{6,7}$ differs by ~50°, $\tau_{11,12}$ by ~40°, and $\tau_{12,13}$ by ~30°. On the other hand, $1U19_B$ gives large R_α and R_β for a nearly planar C12/C13 bond. Similarly, all four molecules in the 1L9H and 1F88 structures give sizable rotational strengths with nearly planar C11/C12 bonds. The cumulative effect of C11/C12 and C12/C13 torsions may be taken into account by means of the dihedral angle Ω_{10-15} between the two planes defined by C10−C11−C12 and C13−C14−C15 (Table 1). The values of Ω_{10-15} for all structures are between 10° and 45°, thus they are more consistent than the various single torsions. The C6/C7 bond consistently shows significant deviations from planarity for all structures. Comparison of the results for $1U19_A$ and $1U19_B$ with those for $1L9H_B$ shows they are very similar despite the fact that $\tau_{6,7}$ differs by nearly a factor of 3. It is interesting to note that the LUMO has little electron density on the atoms of the β-ionone ring (Figure 1), which may account for the insensitivity of the rotational strengths of the α- and β-bands to $\tau_{6,7}$. We conclude that the intrinsic rotational strengths of the α- and β-bands cannot be attributed to the torsion about any one bond in the polyene but must derive from the overall chirality. In fact, the Kohn–Sham orbitals involved in both α- and β-transitions (Figure 1) are similarly localized on a large portion of the molecule, spanning the entire conjugated system from C6 to C15−N. The dependence of computed rotational strengths on the global arrangement of the retPSB chromophore, rather than on any single torsion, also explains the consistency of TDDFT results. Despite the variations observed for some angles, the conformation adopted by the conjugated system is very similar among the various structures considered and defines a right-handed helix (Figure 5). It is the helical character of the retPSB that makes it an inherently chiral chromophore and accounts for the lack of sensitivity to geometric details. Therefore, TDDFT calculations correctly provide a set of consistent CD spectra starting from a coherent ensemble of input structures. As is commonly found, circular dichroism is sensitive to the *overall* absolute conformation: this is the basis for the use of CD in structural analysis but often implies that *specific* geometric quantities cannot be easily disentangled.

Our analysis of the induced CD spectrum of the retPSB chromophore in rhodopsin gives rotational strength contributions that decrease in magnitude in the order: intrinsic > peptide coupling > aromatic coupling. This contrasts with the case for the induced CD of myoglobin and hemoglobin,[102–104] which is: aromatic coupling > peptide coupling > intrinsic. The difference in the relative importance of the intrinsic vs coupling contributions can be rationalized by the intrinsically chiral character of the polyene chain as contrasted to the nearly planar porphyrin. There does not appear to be a simple rationale for the difference in the relative importance of the peptide and aromatic coupling effects.

It should be noted that the dominance of intrinsic rotational strength of the retPSB over coupled-oscillator interactions in rhodopsin may not extend to all retinal-binding proteins, e.g., to bacteriorhodopsin and other archaeal rhodopsins. First, the archaeal rhodopsins have an all-*trans* polyene chromophore that is probably less chiral than the 11-*cis* polyene of rhodopsin. Second, the binding site of the polyene in bacteriorhodopsin appears to be richer in aromatic amino acids than that in rhodopsin, and this may favor larger aromatic coupled-oscillator interactions.

This work validates the assumption of the dominance of inherent chirality to infer the conformation of retPSB in rhodopsin from correlations of the CD of opsin-retinal analogue complexes with that of rhodopsin.[18,38] The methods used here can be applied in combination with MD simulations to simulate the CD of photointermediates in both equilibrium and kinetic studies. Our work also has broader implications for the interpretation of induced CD in other systems, especially those

(102) Hsu, M. C.; Woody, R. W. *J. Am. Chem. Soc.* **1971**, *93*, 3515–3525.
(103) Kiefl, C.; Sreerama, N.; Haddad, R.; Sun, L.; Jentzen, W.; Lu, Y.; Qiu, Y.; Shelnutt, J. A.; Woody, R. W. *J. Am. Chem. Soc.* **2002**, *124*, 3385–3394.
(104) Woody, R. W.; Kiefl, C.; Sreerama, N.; Lu, Y.; Qiu, Y.; Shelnutt, J. A. Molecular dynamics simulations of carbonmonoxy myoglobin and calculations of heme circular dichroism. In *Insulin and Related Proteins − Structure to Function and Pharmacology*; Federwisch, M., Dieken, M. L., De Meyts, P., Eds.; Kluwer Academic: Dordrecht, 2002; pp 233–248.

involving retinoids and carotenoids, in the same way that calculations on myoglobin and hemoglobin CD[102] pointed the way to the interpretation of the CD of heme proteins.

Conclusions

A large positive intrinsic rotational strength is calculated for both the α- and β-bands of the retPSB chromophore of rhodopsin. These intrinsic rotational strengths show limited variability despite significant variations in torsional angles among the structures considered, indicating that the overall chirality of the polyene is more important than torsion about any given bond. The largest coupling contribution is that of the α-band with peptide $\pi\pi^*$ transitions, which is half as large as the intrinsic rotational strength and opposite in sign. The other coupling contributions are substantially smaller. Thus, the intrinsic CD of retPSB is the dominant factor in the induced CD of rhodopsin.

Acknowledgment. Support from the following grants is gratefully acknowledged: NIH GM36564 to N.B. and K.N., NIH EB002803 to N.S. and R.W.W., and FIRB RBPR05NWWC to P.S. and G.P.

Supporting Information Available: Author list for ref 44; Tables S1−S9; Figure S1; Appendix: The method for least-squares adjustment of monopole charges. This material is available free of charge via the Internet at http://pubs.acs.org.

JA711009Y